# SUPPLEMENTAL ONLINE DATA

**Structural and mechanistic insights into the interaction between Pyk2 and Paxillin LD motifs**

Murugendra S. Vanarotti[1], Darcie J. Miller[1], Cristina D. Guibao[1], Amanda Nourse[2] and Jie J. Zheng[1]

[1]Department of Structural Biology, St. Jude Children's Research Hospital, Memphis, Tennessee, USA.

[2]Hartwell Center for Bioinformatics and Biotechnology, St. Jude Children's Research Hospital, Memphis, Tennessee, USA.

# SUPPLEMENTAL FIGURES

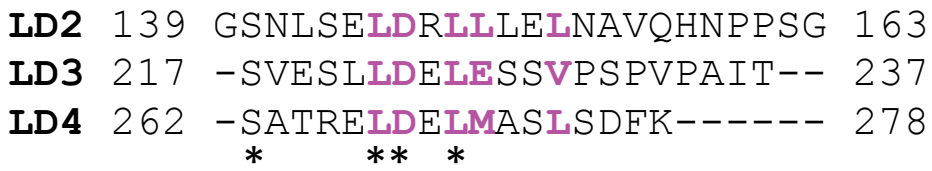


**Figure S1. Paxillin LD motifs sequence comparison**. Sequence alignment of paxillin LD2, LD3 and LD4 peptides used in this study. Identical residues are marked with asterisks, and the LDXLLXXL motif is shown in bold magenta.

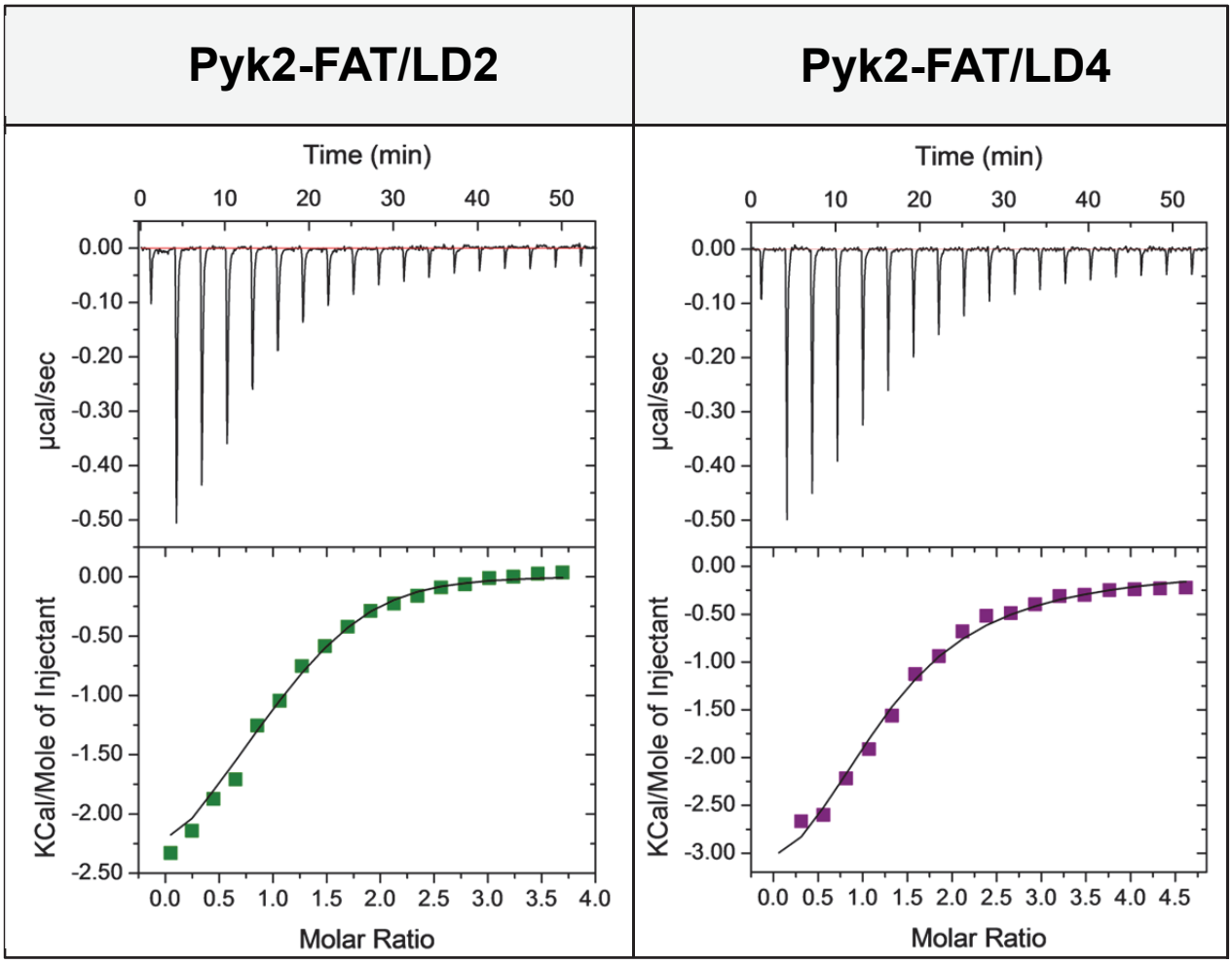


**Figure S2. Isothermal titration calorimetry (ITC) of Pyk2-FAT binding to paxillin LD2 and LD4 peptides.** Isothermal calorimetric titrations of Pyk2-FAT with paxillin LD2 and LD4 peptides in MES buffer at pH 6.2, 298 K. Upper panels show raw data with integration base line (red). Lower panels show data after peak integration and subtraction of blank titrations. The green and purple color boxes in the bottom panels represent the fit to a sequential two-site model for LD2 and LD4 peptides. Thermodynamic parameters are summarized in Table 1.

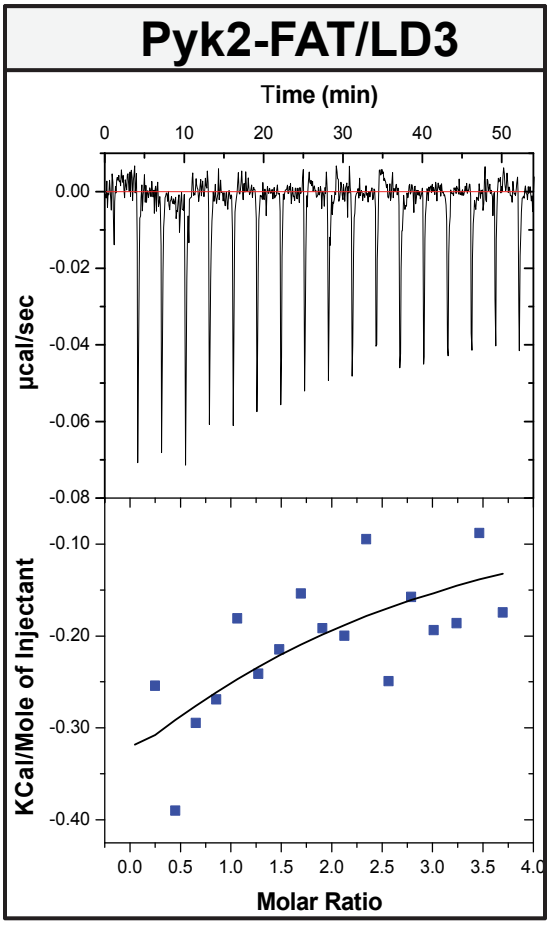


**Figure S3. Isothermal titration calorimetry (ITC) of Pyk2-FAT binding to paxillin LD3 peptide.** Isothermal calorimetric titration of Pyk2-FAT with paxillin LD3 peptide in MES buffer at pH 6.2, 298 K. Upper panels show raw data with integration base line (red). Lower panels show data after peak integration and subtraction of blank titrations. The blue color boxes in the bottom panels represent the fit to a two-site sequential binding model. Because of weak LD3 peptide binding to Pyk2-FAT, the data is not fitting very well.

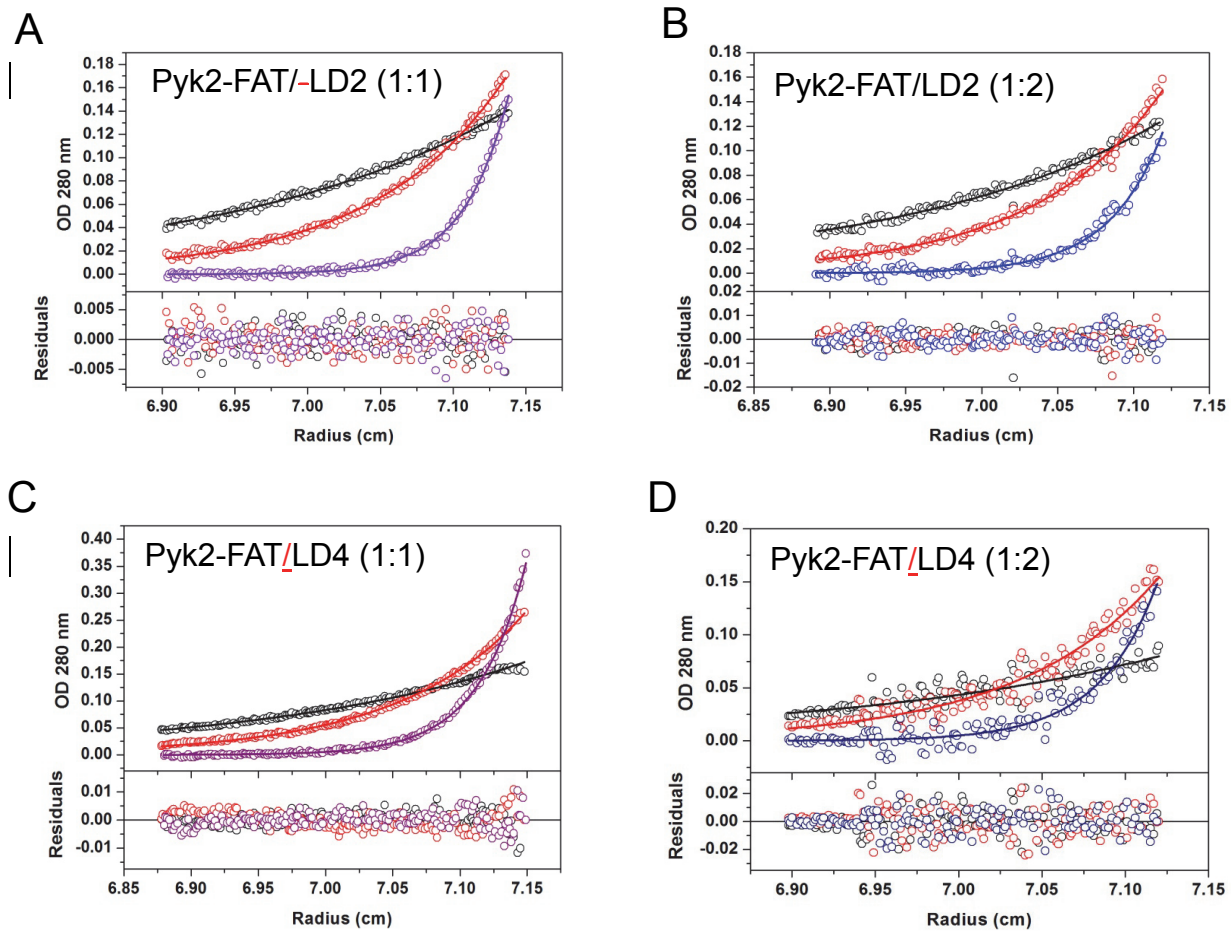


**Figure S4. Sedimentation equilibrium–AUC of Pyk2-FAT/LD2 and Pyk2-FAT/LD4 mixtures.** Absorbance scans at equilibrium are plotted *versus* the distance from the axis of rotation. (A) 1:1 Pyk2-FAT/LD2, (B) 1:2 Pyk2-FAT/LD2, (C) 1:1 Pyk2-FAT/LD4 and (D) 1:2 Pyk2-FAT/LD4 peptide mixtures were centrifuged at 4 °C for 30, 26 and 18 h at each rotor speed of 18.4 (black), 26.9 (red) and 46 k rpm (purple/blue), respectively. The *solid lines* represent the global nonlinear least squares best-fit of all the data sets to a single or two-site heterogeneous association model. Results listed in Table 2A.

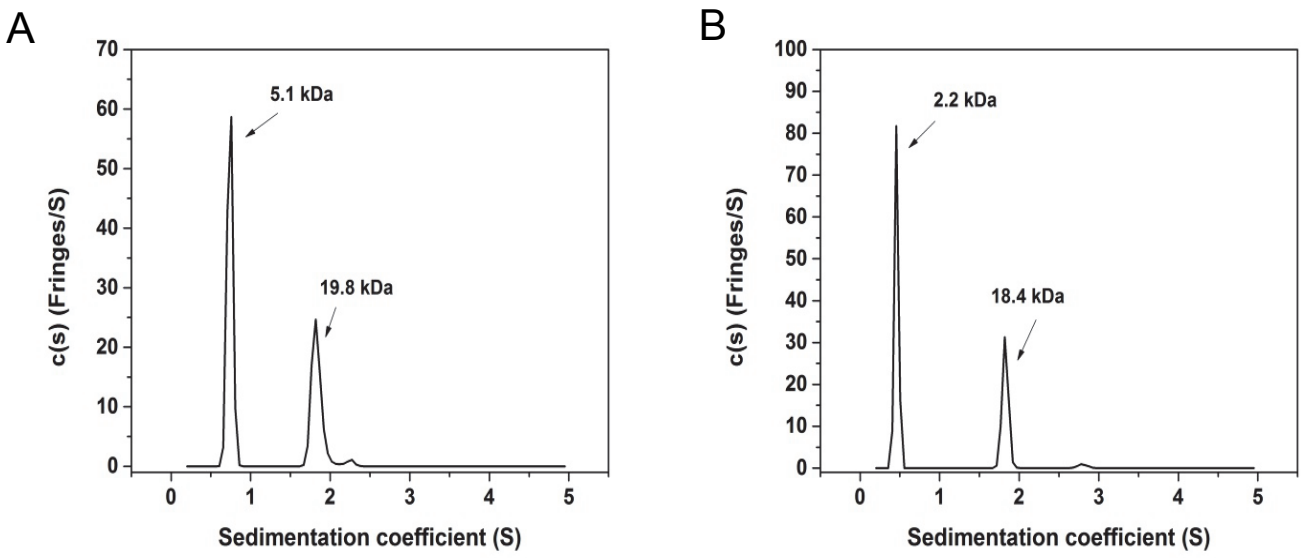


**Figure S5. Analytical Ultracentrifugation Surface Velocity (AUC-SV) of Pyk2-FAT/LD2 and Pyk2-FAT/LD4 complex.** The sedimentation velocity profiles (fringe displacement) were fitted to a continuous sedimentation coefficient distribution model c(s). Mass values for the 2 peaks of the (A) Pyk2-FAT/LD2 complex are 5.1 and 19.8 kDa and for the (B) Pyk2-FAT/LD4 complex are 2.2 and 18.4 kDa. The s and mass values of the proteins are listed in Table S1.

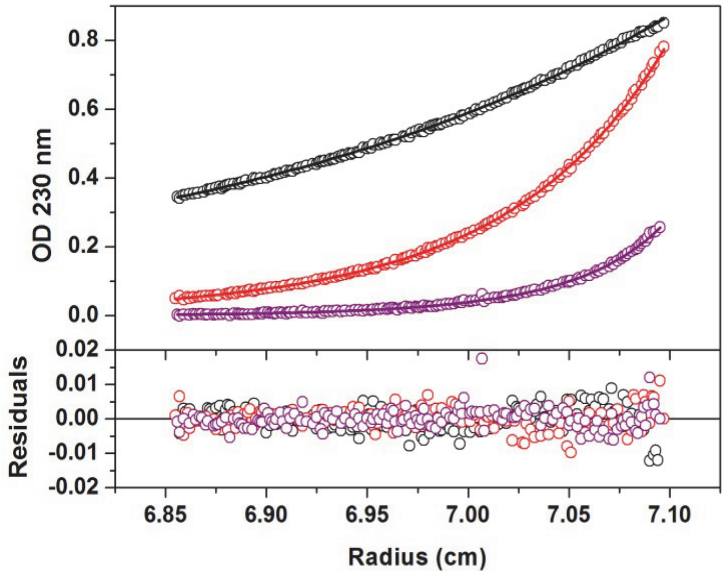


**Figure S6. Sedimentation equilibrium–AUC of Pyk2-FAT and paxillin$^{133\text{-}290}$ mixture**. Absorbance scans at equilibrium are plotted *versus* the distance from the axis of rotation. The Pyk2-FAT and paxillin$^{133\text{-}290}$ mixture was centrifuged at 4 °C for 30, 26 and 18 h at each rotor speed of 18.4 (black), 26.9 (red) and 46 k rpm (purple), respectively. The *solid lines* represent the global nonlinear least squares best-fit of all the data sets to a single or two-site heterogeneous association model. Results listed in Table 2B.

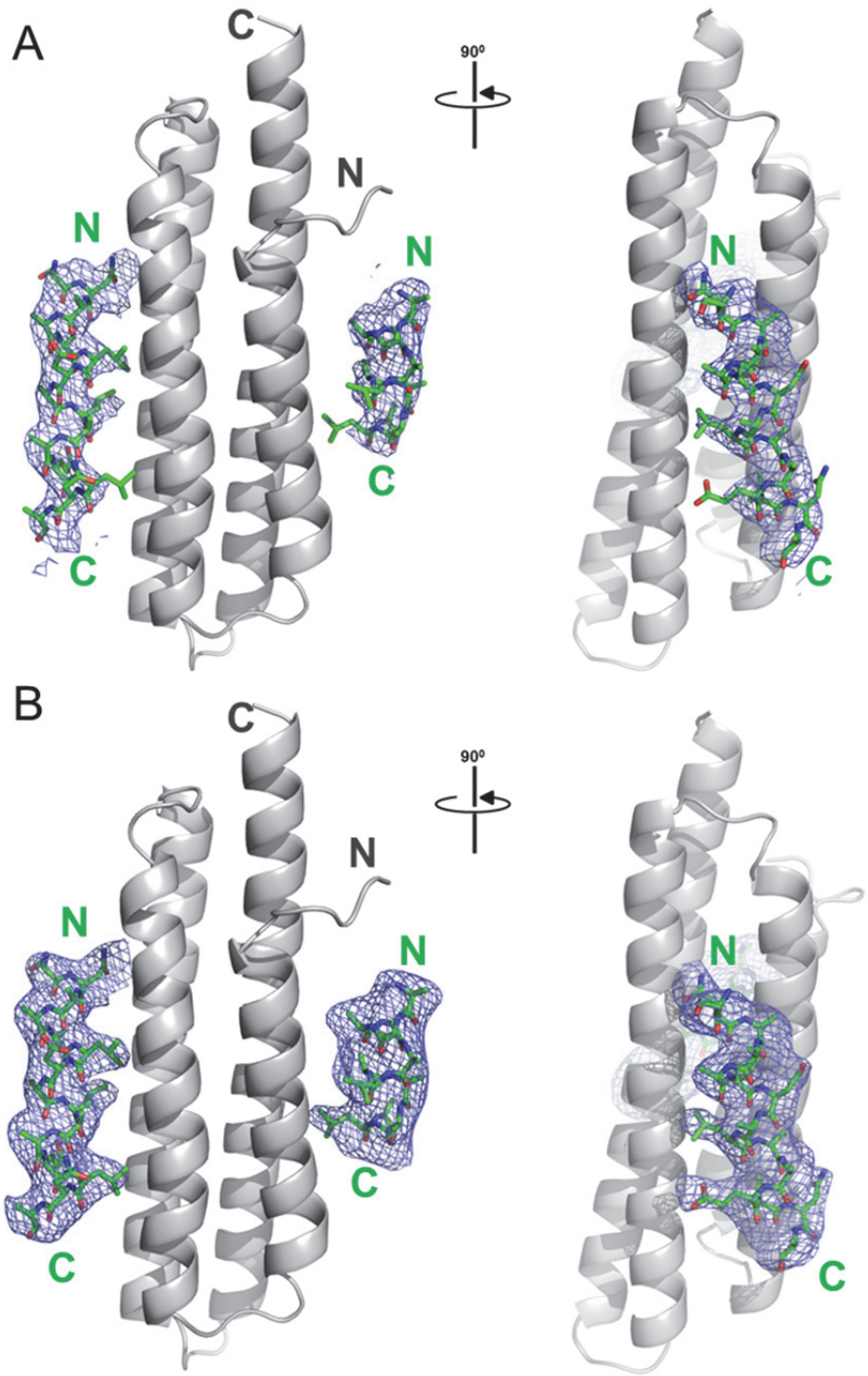


**Figure S7. Electron density maps for LD2 motif peptides.** The Pyk2-FAT domain is colored in grey, and bound LD2 motif peptides are colored in green. (A) DEN refinement (prior to the addition of peptides) Fo-Fc maps contoured at 2.5σ. (B) Final Fo-Fc simulated annealing omit maps for LD2 contoured at 2.5σ.

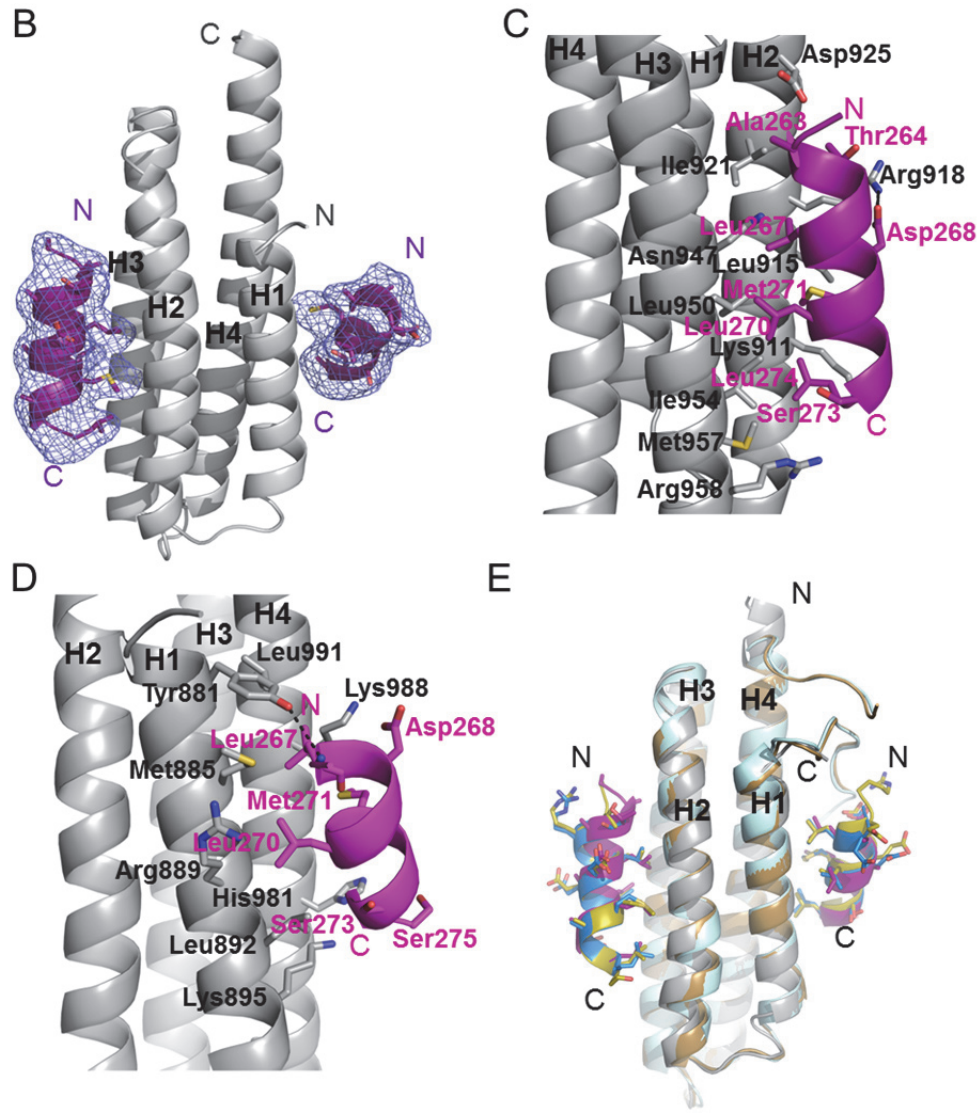


**Figure S8. Structural comparison of Pyk2-FAT bound to paxillin LD4 peptide. (**A) Length of paxillin LD4 peptide used in this study compared with that used by Lulo et al. (PDB: 3GM1) in complex structure determination, labeled in purple and gold respectively. (B, C and D) Pyk2-FAT and paxillin LD4 peptide are colored in grey and purple, respectively. (B) Fo-Fc simulated annealing omit map for Pyk2-FAT/LD4 contoured at 3.0σ. (C and D) Close-up views of the interface between H2/H3 and H1/H4 binding site of Pyk2-FAT and paxillin LD4 peptide. Interacting residues from the LD4 peptide and Pyk2-FAT are shown in sticks with labels colored in purple and black, respectively. Black dotted lines indicate hydrogen bonds. (E) Superposition of our Pyk2-FAT/LD4 complex (PDB: 3U3F) structure (Pyk2-FAT is shown in grey and LD4 peptide in purple) and the previously published Pyk2-FAT/LD4 complex (PDB: 3GM1; Chain A: Pyk2-FAT is show in pale cyan and LD4 peptide in blue, Chain B: Pyk2-FAT is shown in sand and LD4 Peptide in gold).

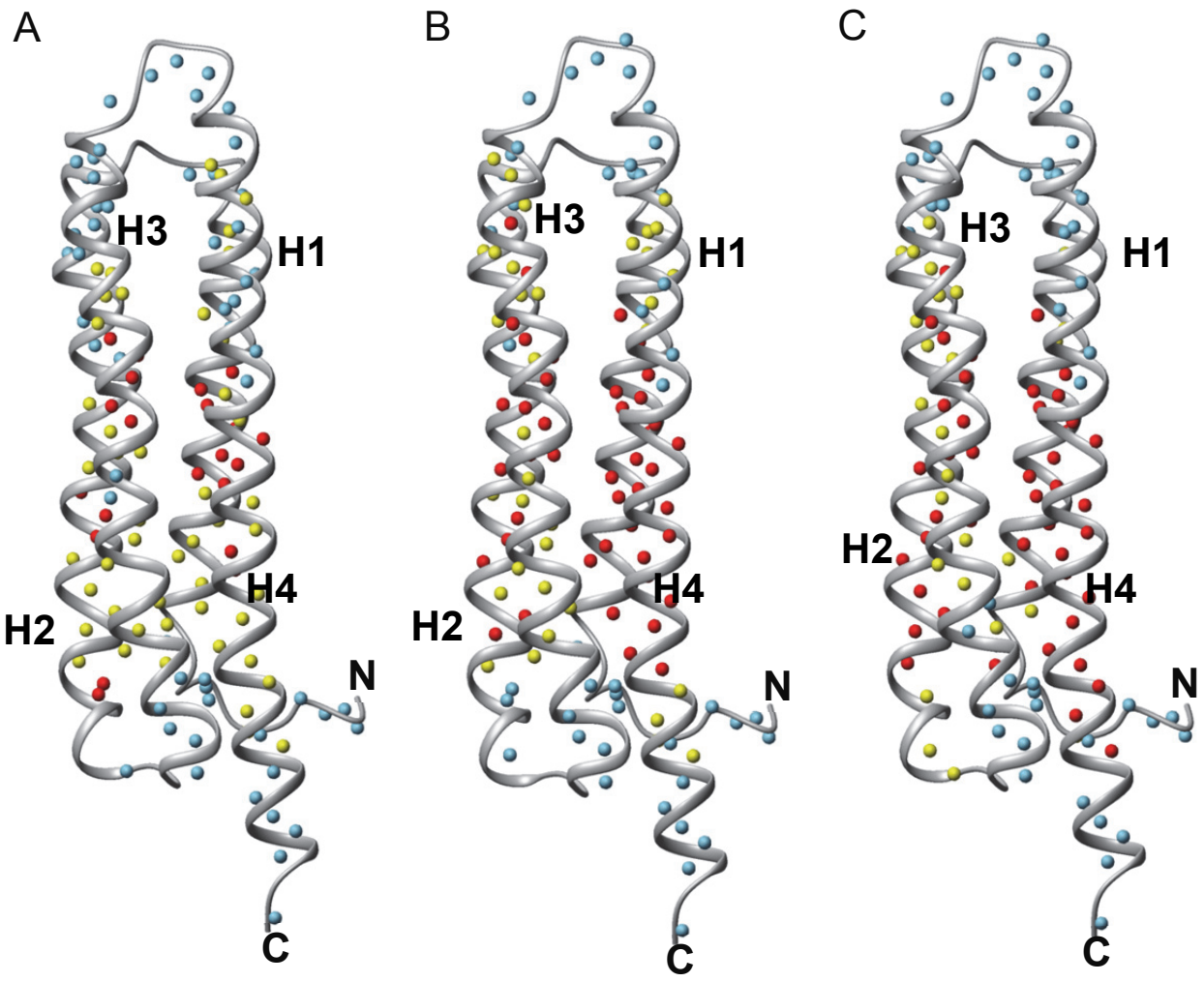


**Figure S9. Hydrogen-deuterium (H/D) exchange.** Representation of H/D exchange experiment on (A) ligand-free Pyk2-FAT, (B) Pyk2-FAT bound to LD2 (1:2) peptide and (C) Pyk2-FAT bound to LD4 peptide (1:2). After the first 10 min, the solvent-exchanged amide proton atoms are colored in light-blue, whereas the protected amide protons are colored in yellow. The atoms that remain protected after 10 hrs are colored in red.

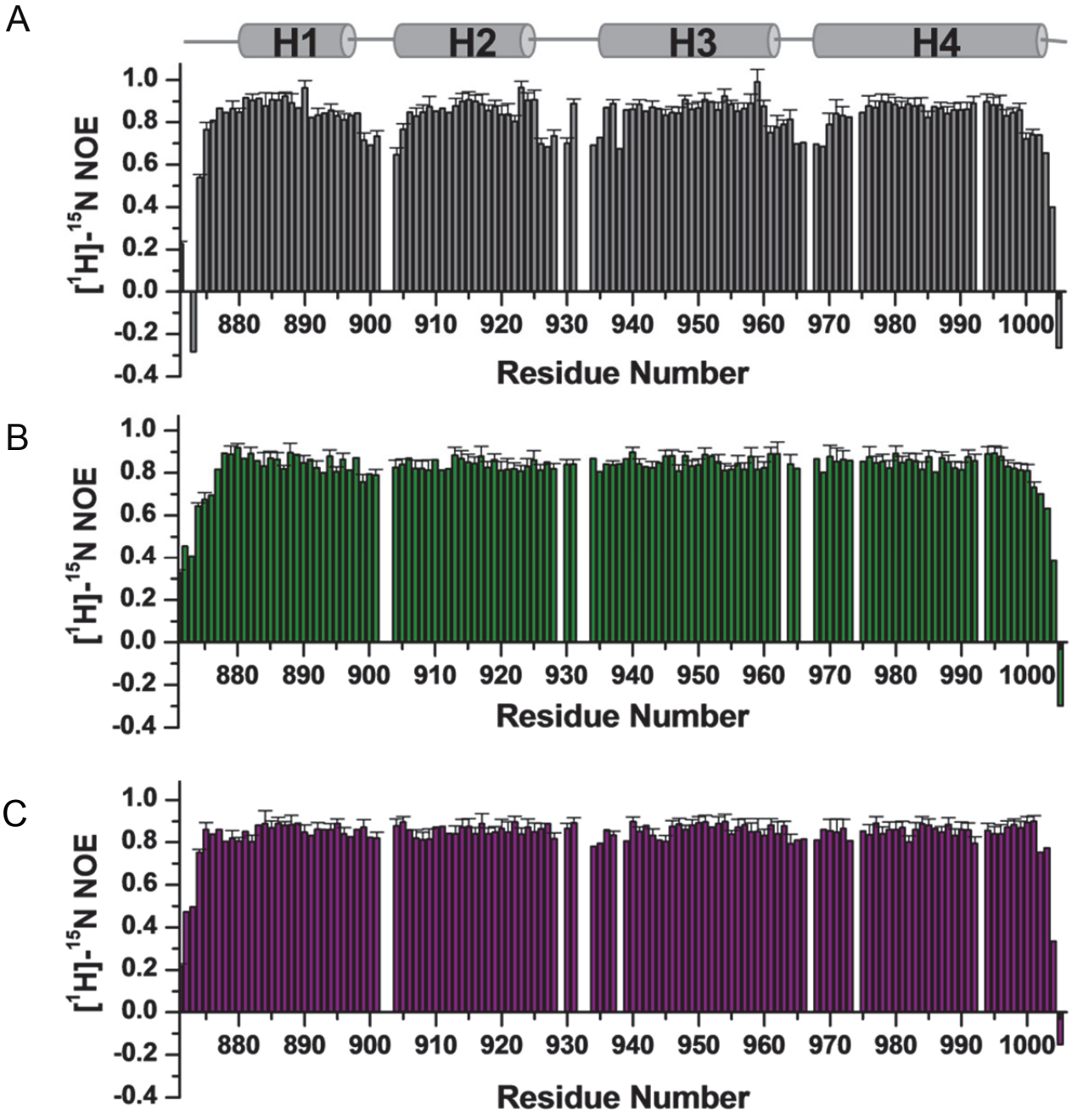


**Figure S10. Plot of backbone amide heteronuclear $^{15}$N-$^{1}$H-NOE values versus residue number for the Pyk2-FAT.** The steady-state heteronuclear $^{15}$N-$^{1}$H-NOE values for (A Free, grey (B) LD2-bound, green and (C) LD4-bound, purple. Pyk2-FAT was plotted versus the residue number measured with a Bruker 600-MHz spectrometer at 25 °C. The secondary structure elements in the Pyk2-FAT are indicated at the top: α-helices 1-4 (H1-H4) were colored in blue, green, red and yellow, respectively. Because the lengths of the N-H bonds are fixed, the $^{15}$N-$^{1}$H-NOE provides information about the dynamics of N-H bonds that can be used to determine whether a particular amide is in a well folded or a flexible region of a protein.

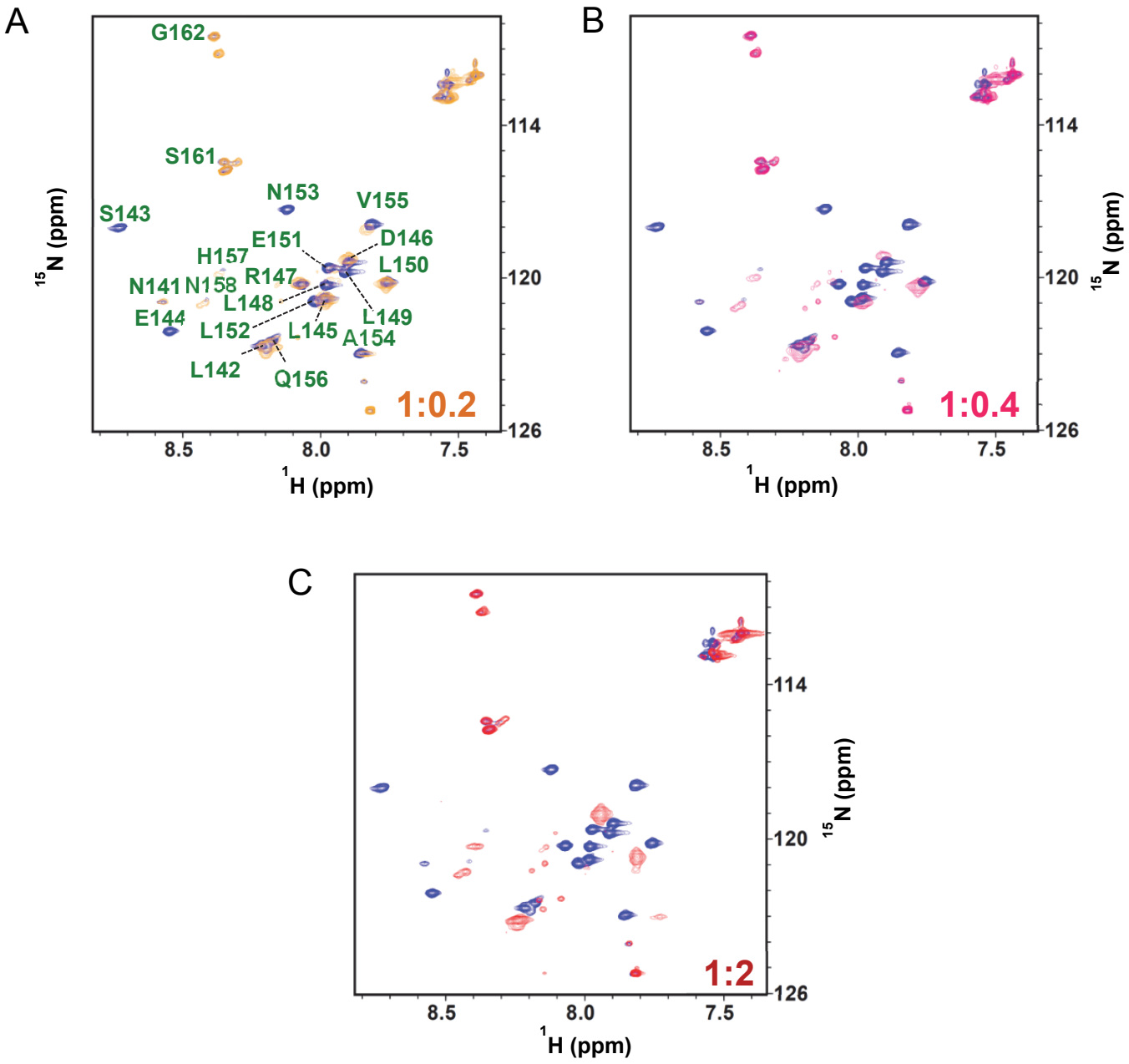


**Figure S11. Mapping the labeled paxillin LD2 and Pyk2-FAT interaction using NMR spectroscopy.** (A-C) $^{13}$C-$^{15}$N-HSQC spectra of 200 μM uniformly labeled paxillin LD2 spectra at different molar ratios of unlabeled Pyk2-FAT were shown in blue (1:0), orange (1:0.2), magenta (1:0.4) and red (1:2). LD2 motif residues are colored in green.

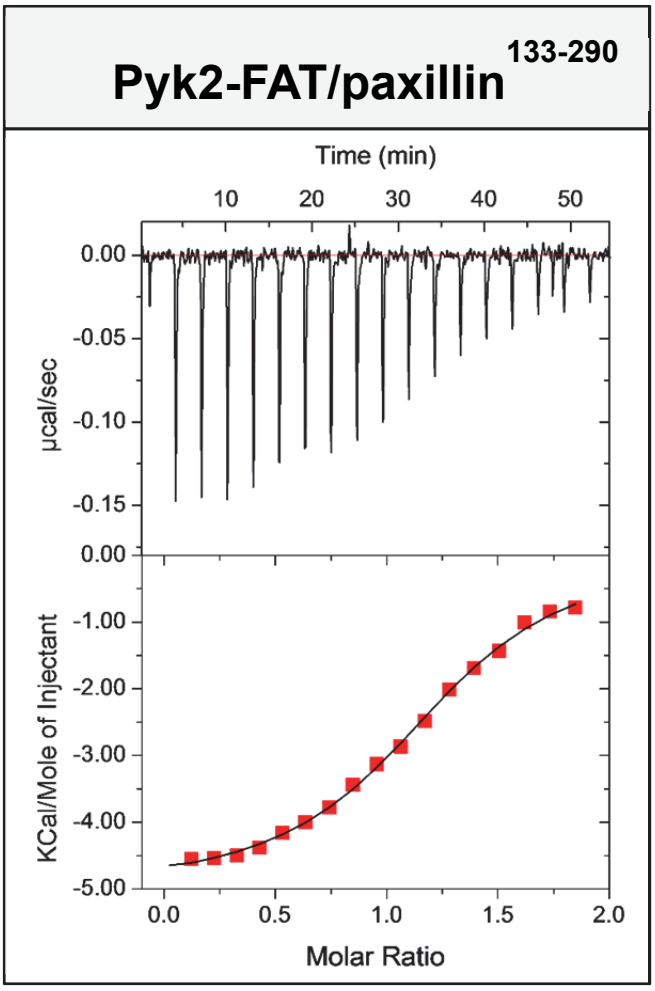


**Figure S12. Isothermal titration calorimetry (ITC) of Pyk2-FAT binding to paxillin$^{133-290}$ constructs.** Isothermal calorimetric titration of Pyk2-FAT with paxillin$^{133-290}$ in MES buffer at pH 6.2, 298 K. Upper panels show raw data with integration base line (red). Lower panels show data after peak integration and subtraction of blank titrations. The red color boxes in the bottom panels represent the fit to a one-site model. Thermodynamic parameters are summarized in Table 1.

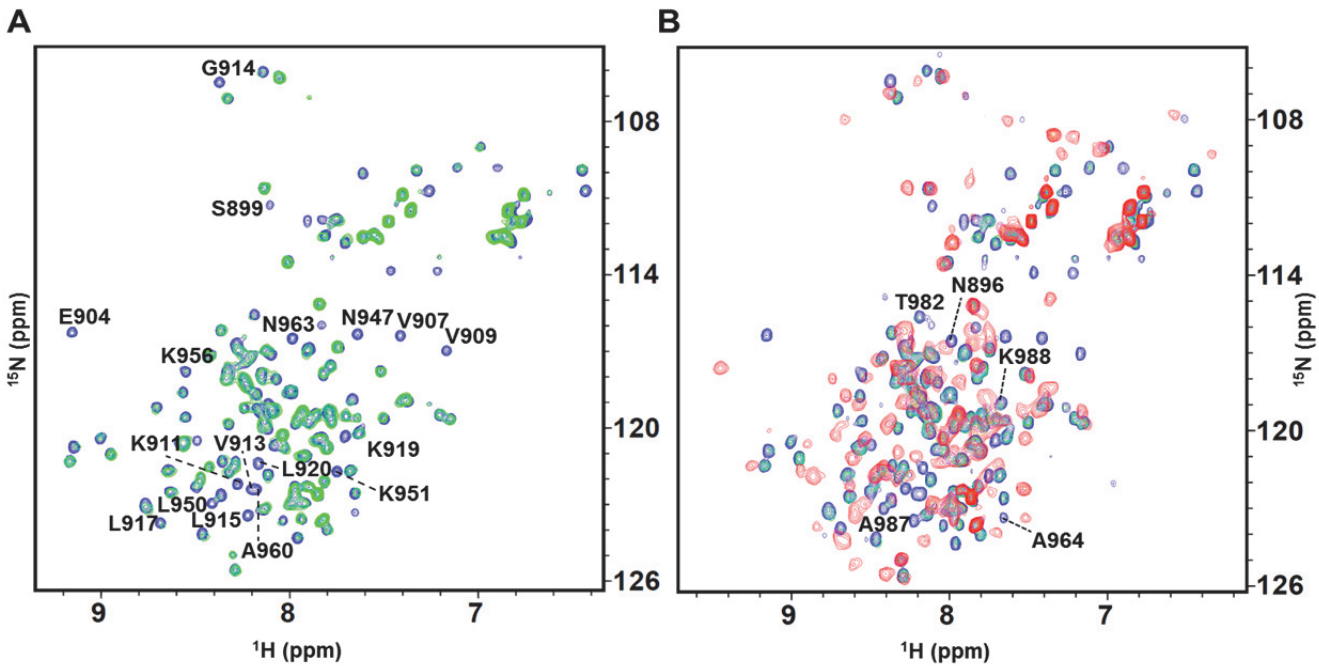


**Figure S13. Binding of paxillin$^{133\text{-}290}$ to Pyk2-FAT H2/H3 and H1/H4 surfaces.** Superposition of $^{1}$H-$^{15}$N TROSY-HSQC spectra of $^{15}$N-labeled Pyk2-FAT in either the absence or presence of the unlabeled paxillin$^{133\text{-}290}$. Spectra acquired at different molar ratios of Pyk2-FAT to paxillin$^{133\text{-}290}$ are shown in blue (1:0), green (1:0.2), cyan (1:0.4), magenta (1:0.8), orange (1:1.2) and red (1:2). (A) Representative residues from H2/H3 of Pyk2-FAT are labeled which undergo intermediate slow exchange after adding paxillin$^{133\text{-}290}$ at low concentrations (1:0.2). (B) Representative residues from H1/H4 of Pyk2-FAT are labeled which undergo fast exchange when paxillin$^{133\text{-}290}$ is added at greater than a 1:0.2 molar ratio.

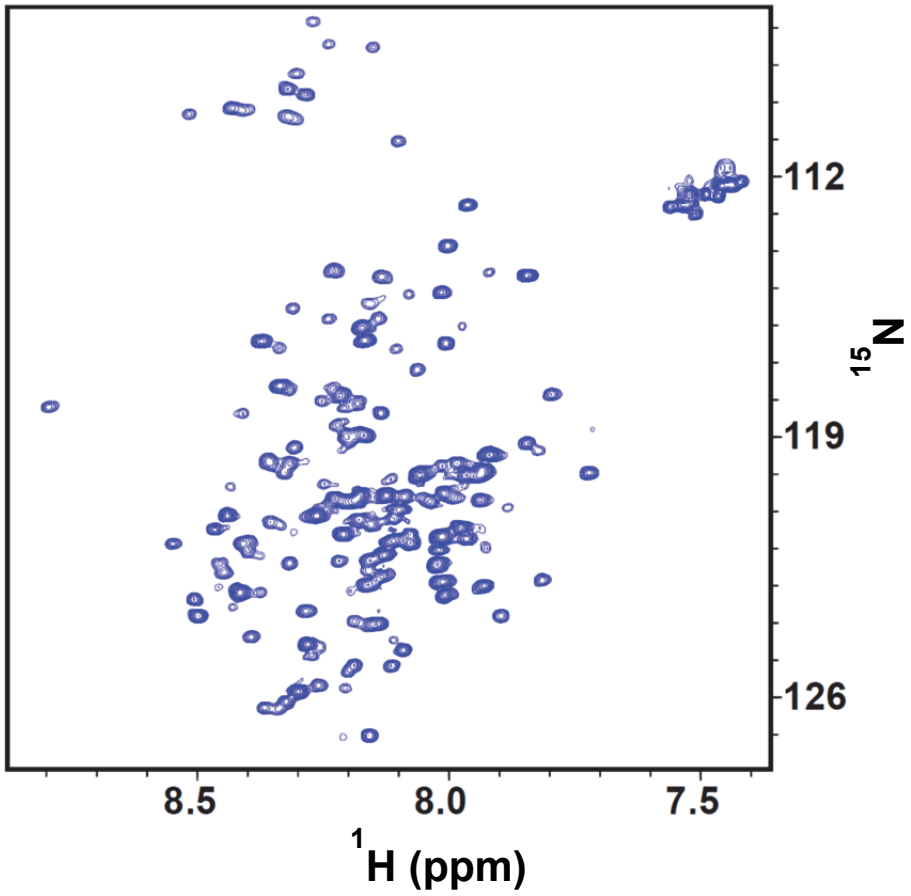


**Figure S14. $^{1}$H-$^{15}$N-TROSY-HSQC spectra of paxillin$^{133-290}$**. 2D $^{1}$H-$^{15}$N- TROSY-HSQC correlation spectra for paxillin$^{133-290}$ showing the characteristics of an intrinsically unstructured protein.

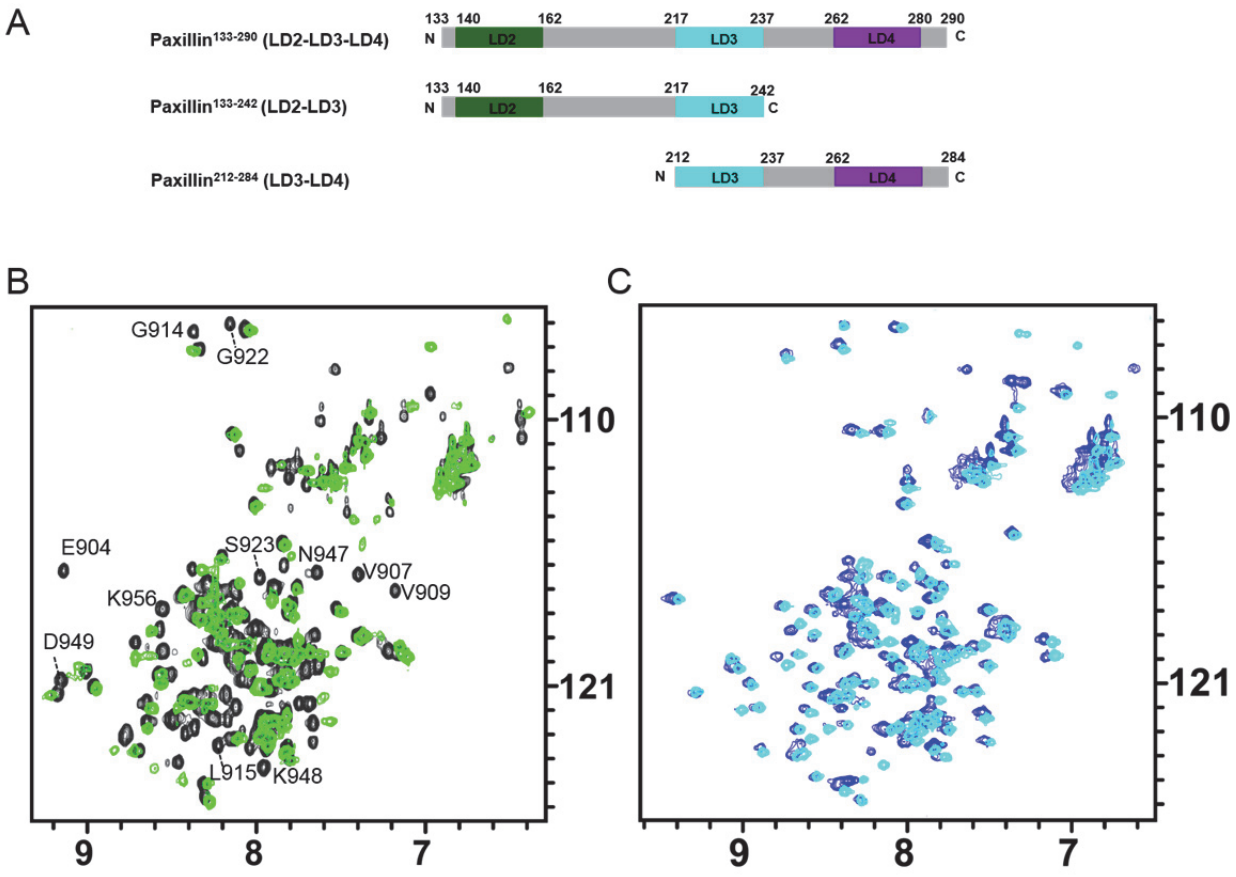


**Figure S15. Pyk2-FAT binding to Paxillin$^{133-242}$ and Paxillin$^{212-284}$.** (A) Schematics of paxillin$^{133-290}$ (LD2-LD3-LD4), paxillin$^{133-242}$ (LD2-LD3) and paxillin$^{212-284}$ (LD3-LD4) constructs. LD2 motif is colored in green, LD3 motif is colored in cyan and LD4 motif is colored in purple. (B) Superposition of $^{1}$H-$^{15}$N HSQC spectra of $^{15}$N-labeled Pyk2-FAT in either the absence or presence of the unlabeled paxillin$^{133-242}$. Spectra acquired at different molar ratios of Pyk2-FAT to paxillin$^{133-242}$ are shown in black (1:0) and green (1:0.4). Representative residues from H2/H3 of Pyk2-FAT are labeled which show chemical shift perturbation when paxillin$^{133-242}$ is added at greater than a 1:0.4 molar ratio. (C) Superposition of $^{1}$H-$^{15}$N HSQC spectra of Pyk2-FAT/paxillin$^{133-242}$ (Blue) and Pyk2-FAT/LD2 (Cyan). These NMR results indicate that the binding mechanism of paxillin$^{133-242}$ (LD2-LD3) and LD2 peptide to Pyk2-FAT appear similar.

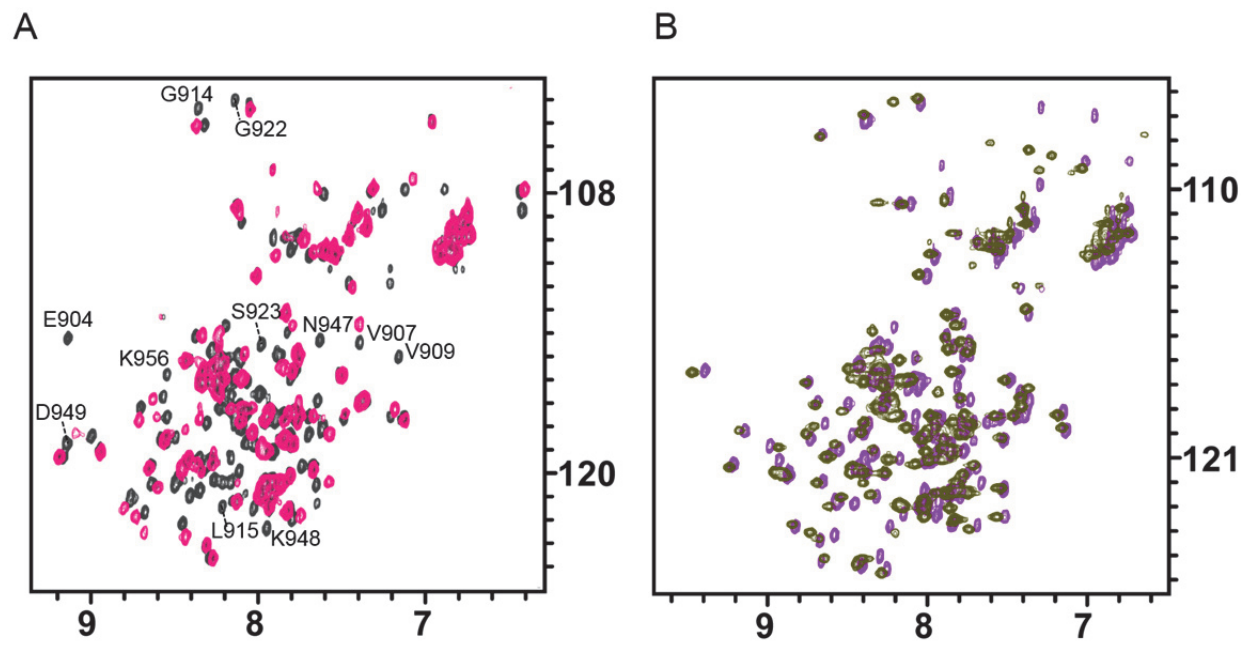


**Figure S16. Paxillin$^{212-284}$ binding to Pyk2-FAT.** (A) Superposition of $^{1}$H-$^{15}$N HSQC spectra of $^{15}$N-labeled Pyk2-FAT in either the absence or presence of the unlabeled paxillin$^{212-284}$. Spectra acquired at different molar ratios of Pyk2-FAT to paxillin$^{212-284}$ are shown in black (1:0) and magenta (1:0.4). Representative residues from H2/H3 of Pyk2-FAT are labeled which show chemical shift perturbation when paxillin$^{212-284}$ is added at greater than a 1:0.4 molar ratio. (C) Superposition of $^{1}$H-$^{15}$N HSQC spectra of Pyk2-FAT/paxillin$^{212-284}$ (Purple) and Pyk2-FAT/LD4 (Olive green). These NMR results indicate the binding mechanism of paxillin$^{212-284}$ (LD3-LD4) and LD4 peptide to Pyk2-FAT appear similar.

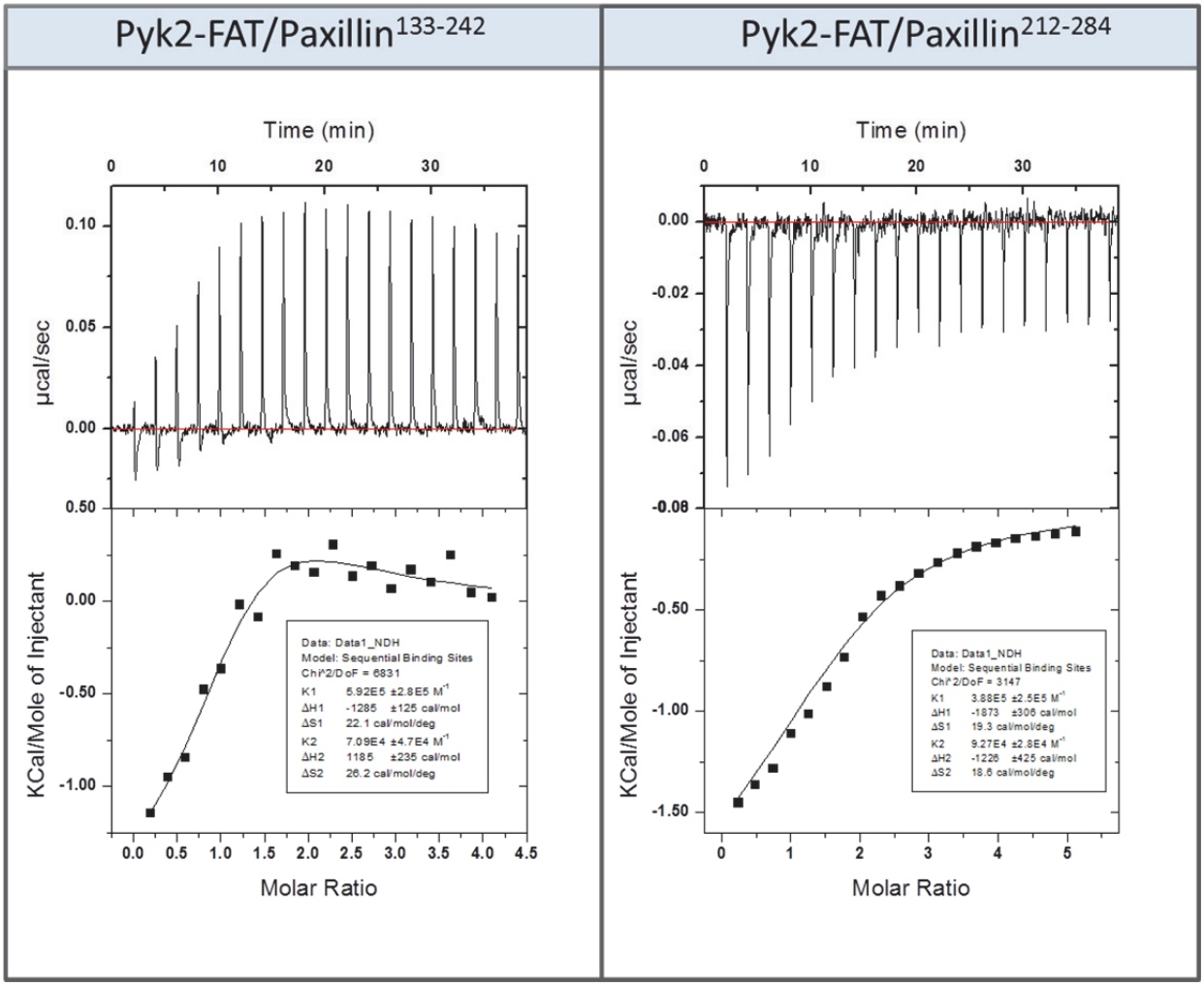


**Figure S17. Isothermal titration calorimetry (ITC) of paxillin$^{133-242}$ and paxillin$^{212-284}$ binding to Pyk2-FAT.** Isothermal calorimetric titrations of Pyk2-FAT with paxillin$^{133-242}$ and paxillin$^{212-284}$ in MES buffer at pH 6.2, 298 K. Upper panels show raw data with integration base line (red). Lower panels show data after peak integration and subtraction of blank titrations. The black color boxes in the bottom panels represent fit to a sequential two-site model for paxillin$^{133-242}$ and paxillin$^{212-284}$. Thermodynamic parameters are summarized in Table S2.

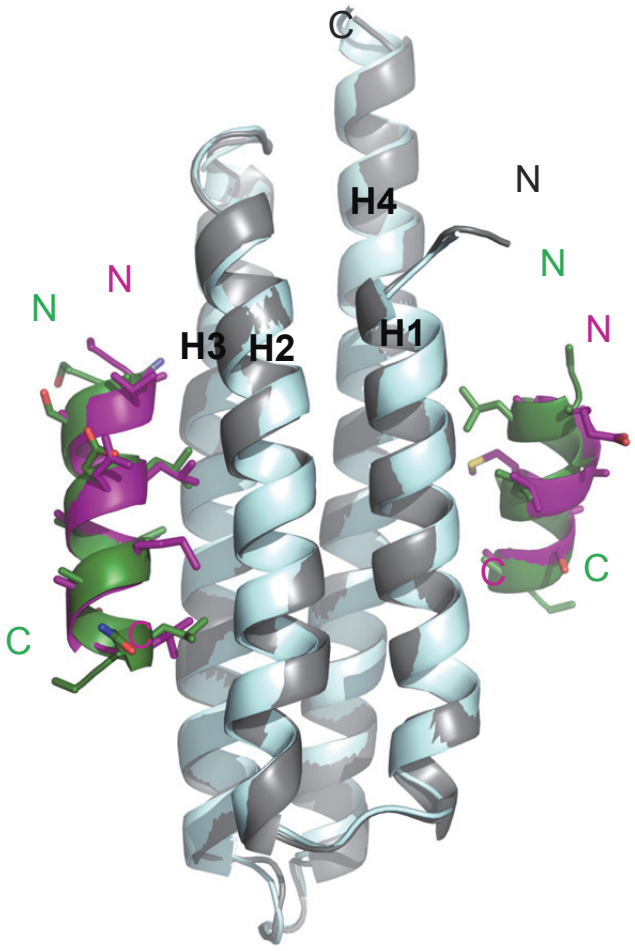


**Figure S18 Comparison of the Pyk2-FAT/LD2 and Pyk2-FAT/LD4 complex crystal structures.** Superposition of our Pyk2-FAT/LD2 and Pyk2-FAT/LD4 complex crystal structure (PDB: 3U3F) shown in gray and pale cyan, respectively. Bound LD2 peptides are shown in green and LD4 peptides in purple.

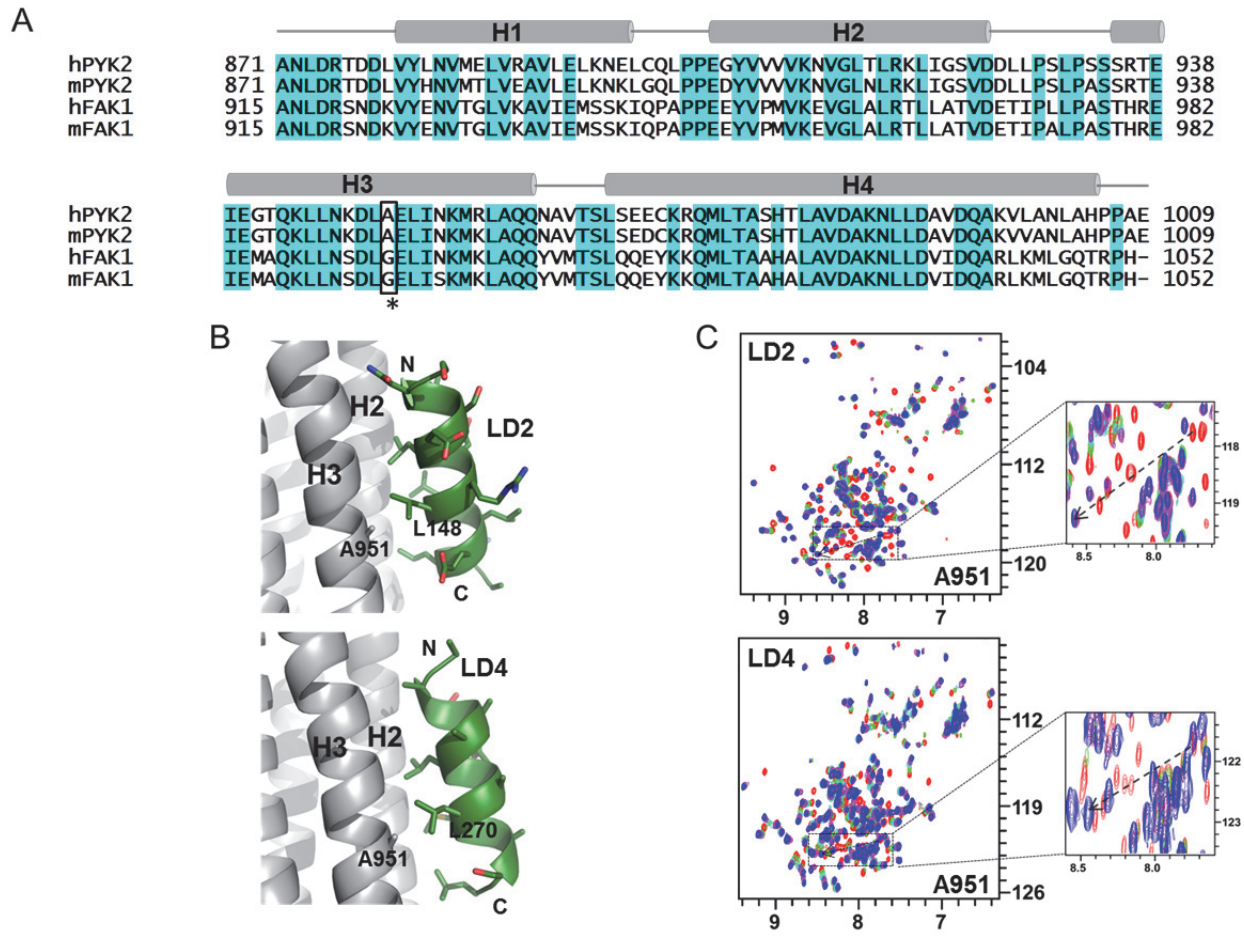


**Figure S19. Comparison of Pyk2-FAT and FAK-FAT binding to paxillin LD2 and LD4 peptides.** (A) Structure-based sequence alignment of FAT domain of Pyk2 with FAT domain of FAK. Human Pyk2 residues 871–1009 (SwissProt Q14289), mouse Pyk2 residues 871-1009 (SwissProt Q9QVP9), human FAK residues 915–1052 (SwissProt Q05397), and mouse FAK residues 915-1052 (SwissProt P34152) are shown. Conserved residues are highlighted in cyan. Ala 951 of Pyk2-FAT and Gly 995 of FAK-FAT are shown in black box with asterisk. (B) In Pyk2-FAT/LD2 and Pyk2-FAT/LD4 structures, Ala 951 is in close proximity to make hydrophobic interaction with Leu 148 and Leu 270 of LD2 and LD4 peptides, respectively. This hydrophobic interaction is missing in FAK-FAT, where alanine is replaced by a glycine (Gly 995). (C) Superposition of $^{1}H$-$^{15}N$ HSQC spectra of Pyk2-FAT at different molar ratios of LD2 and LD4 peptides shows that Ala 951 undergoes the highest NMR chemical shift perturbation upon peptide binding. $^{1}H$-$^{15}N$ HSQC spectra of Pyk2-FAT at different molar ratios of LD2 and LD4 peptide are colored in red (1:0), green (1:0.2), cyan (1:0.4), purple (1:0.8), magenta (1:1.2) and blue (1:2).

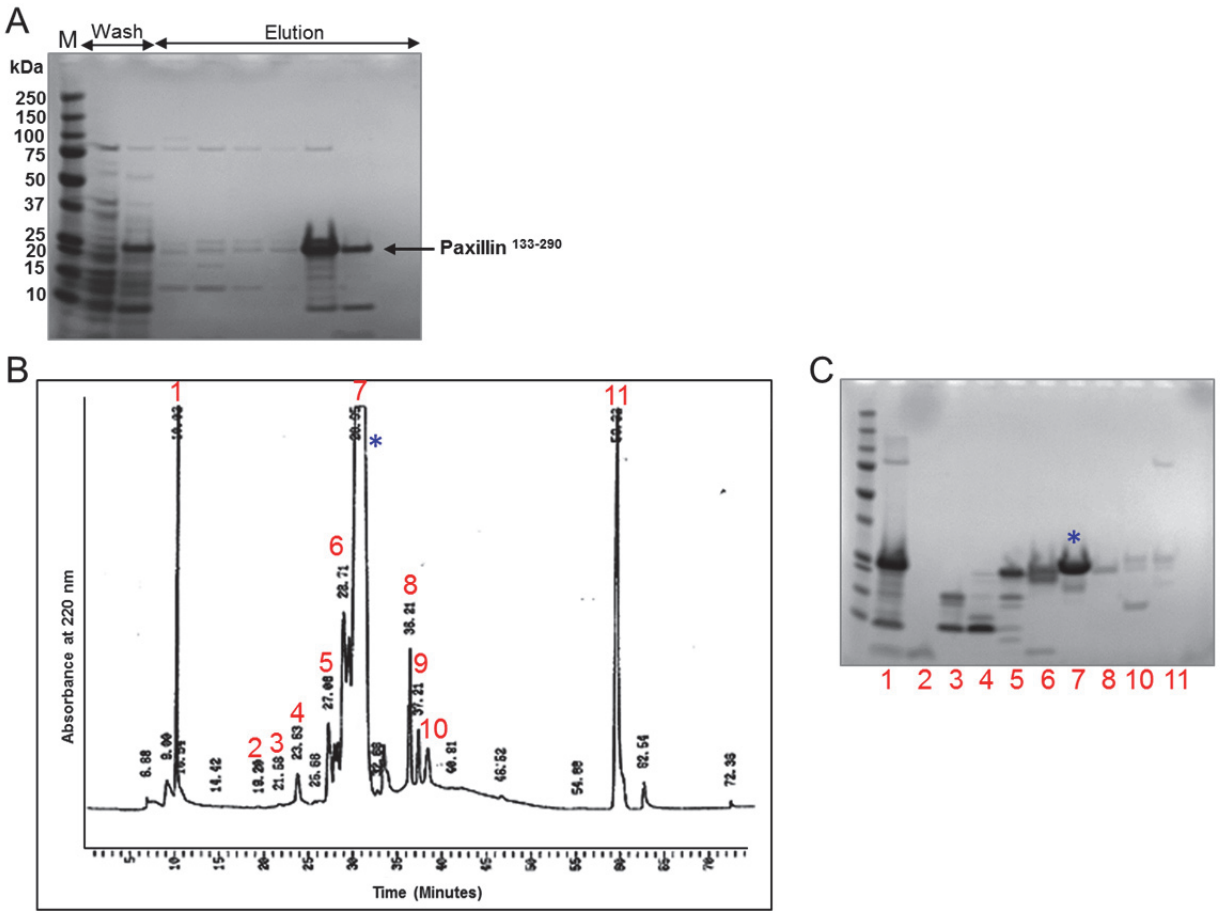


**Figure S20. Expression and purification of the paxillin$^{133-290}$.** (A) SDS-PAGE of purified paxillin$^{133-290}$ from nickel affinity column. Paxillin$^{133-290}$ was eluted at 200 mM imidazole concentration. (B) HPLC-chromatogram of paxillin$^{133-290.}$ Eluted peaks were labeled from 1 to 11. (C) SDS-PAGE of HPLC purified fractions. Fraction 7 is paxillin$^{133-290}$.

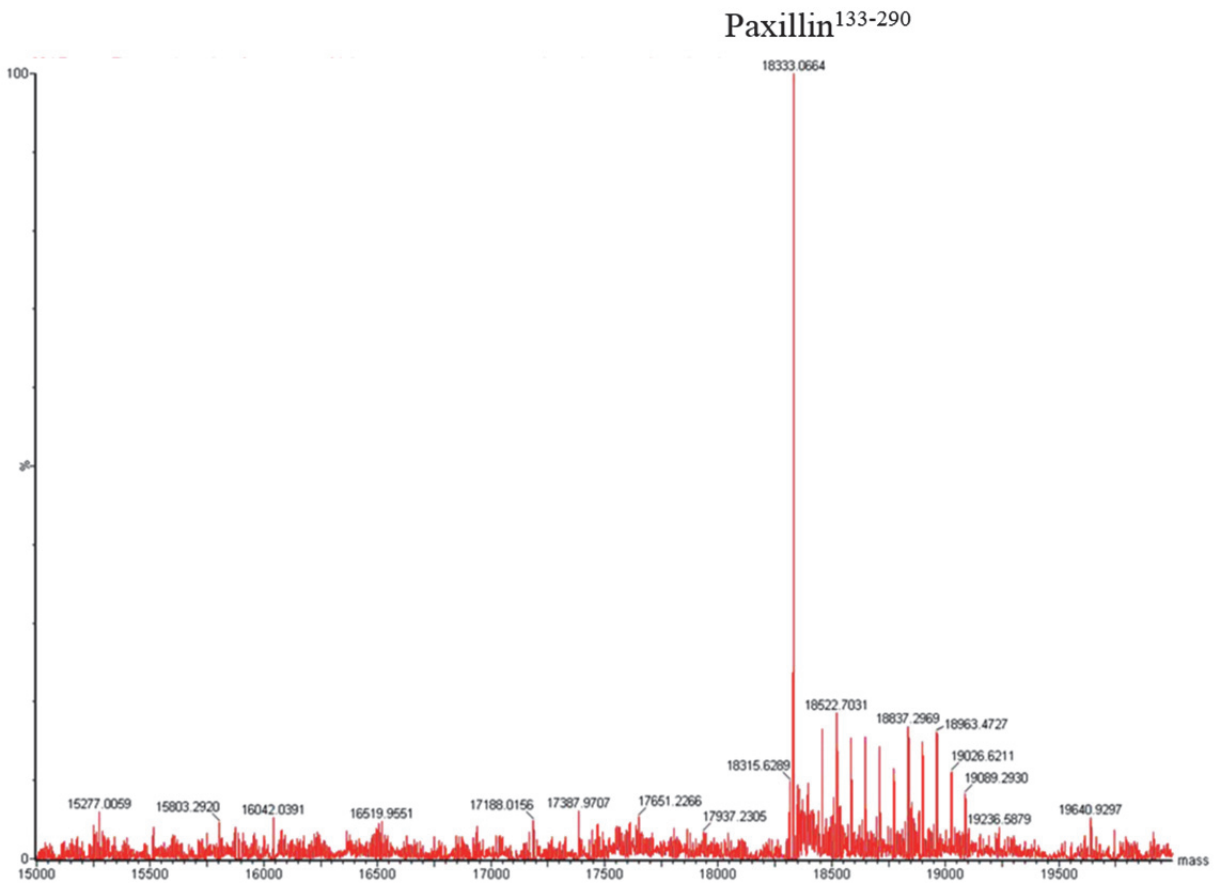


**Figure S21. MALDI-TOF spectra of the paxillin$^{133\text{-}290}$.** The theoretical mass of paxillin$^{133\text{-}290}$ is 18,377.30 Da, and the peak corresponding to the protein is observed at m/z 18,333.06, which is ~44 Da lower than the theoretical mass of the protein. This difference may arise from C-terminal decarboxylation. Carboxylic acids tend to fragment by losing a molecule of carbon dioxide, CO2, which is equivalent to a loss of 44 Da.

# SUPPLEMENTAL TABLES

## Table S1: Analytical Ultracentrifugation Sedimentation velocity (AUC-SV) experiments.

| Sample | mg/ml [a] | $s_{20}$ (Svedberg) [b] | $s_{20,w}$ (Svedberg) [c] | Mw (kDa) [d] | $f/f_0$ [e] |
|---|---|---|---|---|---|
| **Pyk2-FAT+LD2** | 2.4 | 0.74 (60%)<br>1.83 (38%) | 0.75<br>1.86 | 5.10<br>19.8 | 1.41 |
| **Pyk2-FAT+LD4** | 2.1 | 0.45 (64%)<br>1.82 (36) | 0.46<br>1.85 | 2.24<br>18.4 | 1.35 |

*a*. Total loading concentration in mg/ml.
*b*. Sedimentation coefficient taken from the ordinate maximum of each peak in the best-fit *c(s)* distribution at 20 °C with percentage protein amount in parenthesis. Sedimentation coefficient (*s*-value) is a measure of the size and shape of a protein in a solution with a specific density and viscosity at a specific temperature.
*c*. Standard sedimentation coefficient in water at 20 °C.
*d*. Molecular mass values taken from the *c(s)* distribution that was transformed to the *c(M)* distribution.
*e*. Best-fit weight-average frictional ratio values $(f/f_0)_w$ taken from the *c(s)* distribution.

## Table S2: Thermodynamic parameters for binding of paxillin$^{133-242}$ and paxillin$^{212-284}$ to Pyk2-FAT obtained by ITC.

| | Pyk2-FAT Domain | | | |
|---|---|---|---|---|
| | Site (n) [a] | $K_D$ (µM) [b] | ΔH [b] | -T.ΔS [b] |
| | | | kcal/mol | |
| **Paxillin$^{133-242}$** | First<br>Second | 1.7±0.55<br>14±5.6 | -1.3±0.1<br>1.2±0.2 | -6.6<br>-7.8 |
| **Paxillin$^{212-284}$** | First<br>Second | 2.6±1<br>11±2.5 | -1.9±0.3<br>-1.2±0.4 | -5.8<br>-5.5 |

*a*. Binding stoichiometry.
*b*. $K_D$ is the dissociation constant. ΔH and ΔS are the change is enthalpy and entropy upon binding at T=298 K, respectively.